The Nitrogen-absorption Isotherm for Fe-21.5at.%Cr Alloy: Uptake of Excess Nitrogen in Dependence on the Precipitation Morphology

Santosh Hosmani, Ralf Schacherl, Lidia Lityńska-Dobrzyńska, Eric Jan Mittemeijer

The Nitrogen-absorption Isotherm for Fe-21.5at.%Cr Alloy: Uptake of Excess Nitrogen in Dependence on the Precipitation Morphology

Journal:	*Philosophical Magazine & Philosophical Magazine Letters*
Manuscript ID:	TPHM-08-Feb-0056.R1
Journal Selection:	Philosophical Magazine
Date Submitted by the Author:	02-Jul-2008
Complete List of Authors:	Hosmani, Santosh; Max Planck Institute for Metals Research, Prof. Dr Ir. E.J. Mittemeijer Schacherl, Ralf; University of Stuttgart, Institute of Physical Metallurgy Lityńska-Dobrzyńska, Lidia; Polish Academy of Sciences, Institute of Metallurgy and Materials Science Mittemeijer, Eric Jan; Max Planck Institute for Metals Research, Prof. Dr Ir. E.J. Mittemeijer
Keywords:	microstructure, nitrides, phase transformations, precipitation
Keywords (user supplied):	iron alloys, excess nitrogen

Philosophical Magazine

ARTICLE TYPE [ORIGINAL PAPER / MANUSCRIPT (REGULAR ARTICLE)]

Article Title [The Nitrogen–absorption Isotherm for Fe-21.5at.%Cr Alloy: Uptake of Excess Nitrogen in Dependence on the Precipitation Morphology]

The Nitrogen–absorption Isotherm for Fe-21.5at.%Cr Alloy: Uptake of Excess Nitrogen in Dependence on the Precipitation Morphology

Santosh S. Hosmani[a]; Ralf E. Schacherl[b*]; Lidia Lityńska-Dobrzyńska[c] and Eric J. Mittemeijer[a, b]

[a] *Max Planck Institute for Metals Research, Heisenbergstr. 3, D-70569 Stuttgart, Germany;*

[b] *Institute for Physical Metallurgy, University of Stuttgart, Germany;*

[c] *Institute of Metallurgy and Materials Science, Polish Academy of Sciences, Reymonta Street 25, 30-059 Cracow, Poland*

Correspondence address:

Dr. Ralf E. Schacherl
Institute for Physical Metallurgy, University of Stuttgart,
Heisenbergstr. 3, D-70569 Stuttgart
Germany

Tel: +49-711-6893314 Fax: +49-711-6893312
e-mail: r.schacherl@mf.mpg.de

E-mail addresses of all authors:

Dr. Santosh S. Hosmani *(s.hosmani@mf.mpg.de)*
Dr. Ralf E. Schacherl *(r.schacherl@mf.mpg.de)*
Dr. Lidia Lityńska-Dobrzyńska *(nmlityns@imim-pan.krakow.pl)*
Prof. Dr. Ir. Eric J. Mittemeijer *(e.j.mittemeijer@mf.mpg.de)*

[*] Corresponding author. Email: r.schacherl@mf.mpg.de

Abstract

Nitriding of Fe-21.5at.%Cr alloy leads to a "discontinuously coarsened", chromium-nitride/ferrite lamellar precipitation morphology in the nitrided zone. The nitrogen-absorption isotherm for this alloy with this precipitation morphology was determined at 560 °C. To assure a constant precipitation morphology the Fe-21.5at.%Cr specimen was first homogeneously pre-nitrided (at 580 ºC in an ammonia/hydrogen gas mixture of nitriding potential of 0.103 $atm^{-1/2}$) and then de-nitrided (at 470 ºC in hydrogen gas atmosphere). The amount of nitrogen remaining in the de-nitrided specimen indicated that the composition of the nitride precipitates is CrN and not (Fe, Cr)N. The measured nitrogen-absorption isotherm revealed the presence of excess nitrogen in the nitrided specimen, which is a surprise in view of the coarse, lamellar precipitation morphology. The occurrence of this excess nitrogen could be ascribed to an unexpected, minor fraction of the total chromium content in the alloy present as coherent, tiny nitride platelets within the ferrite lamellae of the "discontinuously coarsened" lamellar precipitation morphology, as evidenced by transmission electron microscopy. A possible kinetic background for this unusual phenomenon was discussed.

Keywords: iron alloys; microstructure; precipitation; nitrides; excess nitrogen

1. Introduction

Nitriding is the most versatile thermochemical surface treatment of ferritic steels, as it can lead, dependent on tuning of the nitriding-process parameters, to pronounced improvements of the fatigue, wear and anti-corrosion properties [1, 2]. *Gaseous* nitriding, as compared to plasma and salt-bath process variants, has the eminent advantage of allowing precise control of the chemical potential of nitrogen in the nitriding atmosphere via the gas flow rates, in fact the partial pressures, of ammonia and hydrogen, i.e. via the so-called nitriding potential, r_n ($=p_{NH_3}/p_{H_2}^{3/2}$, with p as partial pressure) [3, 4].

Chromium is often used as alloying element in ferritic nitriding steels because of its affinity for nitrogen, leading to the precipitation of CrN in the nitrided zone. Nitriding of iron-based alloys containing Cr was subject of several investigations [5–18]. The microstructure of gaseous nitrided Fe-Cr alloys containing a low concentration of chromium (say, less than about 1wt.% or below) shows a "continuous" precipitation morphology due to coherent, submicroscopical CrN platelets in the nitrided zone [10, 11, 19]. Two precipitation morphologies, "continuous" and "discontinuous", occur in the nitrided zone of Fe-Cr alloys containing an amount of chromium in the range 2 – 13 wt.% Cr [6–9]. "Discontinuous" means the result of a discontinuous coarsening reaction occurring for the initially "continuous" precipitate microstructure: a lamellar, CrN / α-Fe precipitation morphology [5, 6, 12, 20]. The nitrided zone of Fe-Cr alloys containing a high amount of chromium, say 13wt.% or above (e.g., see [8]), consists of grains exhibiting only the "discontinuous" precipitation morphology: the relatively low migration rate for the nitriding front, in the alloys with relatively high chromium content, allows the discontinuous coarsening reaction front to catch up with the nitriding front [21]. The driving force for the discontinuous coarsening reaction is the relaxation of internal strain fields, and reduction of the interfacial area between

precipitates and matrix and of the nitrogen supersaturation [5, 20]. Discontinuous coarsening leads to a pronounced decrease of hardness [6].

Nitrided Fe-Cr alloys contain more nitrogen than necessary for (i) precipitation of all chromium as nitride, $[N]_{CrN}$, and (ii) equilibrium saturation of the ferrite matrix, $[N]_{\alpha}^{0}$; i.e. "excess nitrogen" has been taken up [6–9]. It has been suggested that a significant part of the excess nitrogen in nitrided binary iron-based alloys is adsorbed at the (coherent) nitride/matrix interfaces, $[N]_{interface}$ [22–26]. $[N]_{interface}$ does not take part in the diffusion process and therefore has been called "immobile" excess nitrogen [8]. The other part of excess nitrogen consists of nitrogen dissolved interstitially in the ferrite matrix (enhanced nitrogen lattice solubility) due to the positive volume misfit between the (coherent) nitride particles and the iron matrix which causes a dilatation of the matrix lattice, $[N]_{strain}$ [22]. The nitrogen corresponding to $[N]_{strain}$ can take part in the diffusion process and therefore has been called "mobile" excess nitrogen [8]. The excess nitrogen (immobile and mobile), as discussed above, is a consequence of the "continuous" precipitation morphology. Therefore it is of interest to analyse the nitrogen uptake in high chromium Fe-Cr alloys which only show the "discontinuous" precipitation morphology. Nitrogen-absorption isotherms (i.e. the amount of nitrogen taken up by a homogeneously nitrided specimen as a function of the nitriding potential) have been fruitfully used to analyse nitrogen uptake in Fe-Al [23, 27], Fe-Ti [25], Fe-V [28] and Fe-Cr [19] alloys; in all these cases only a "continuous" precipitation morphology occurred. In this work the nitrogen-absorption isotherm for Fe-21.5at.%Cr alloy, exhibiting the "discontinuous" precipitation morphology, was investigated.

2. Experimental

The Fe-21.5at.%Cr alloy was prepared from pure Fe (99.98 wt.%) and pure Cr (99.999 wt. %) in an Al_2O_3 crucible in an inductive furnace under an argon atmosphere (99.999 vol. %). The amounts

of chromium and light element impurities in the alloy (see table 1) were determined by chemical analysis (inductive-coupled plasma-optic emission spectroscopy).

The alloy cast was cold rolled to a sheet of 1.0 mm thickness. Specimens with lateral dimensions of 1.0 cm X 2.0 cm were cut from the sheet. These specimens were encapsulated in a silica tube filled with argon. The encapsulated specimens were recrystallized at 700 ºC for 2 h. The recrystallized specimens were ground and polished to remove any oxide layer formed on the surface. Thereafter, each specimen was subjected to cold rolling to obtain thin foils of about 0.30 mm thickness. Specimens with lateral dimensions of 1.0 cm X 1.5 cm were cut from the foils. These thin foil specimens were recrystallized at 700 ºC for 2 h. The recrystallized thin foil specimens were ground, polished (last step: 1 µm diamond paste) and cleaned in an ultrasonic bath filled with ethanol.

To start the nitriding process the specimen was suspended at a quartz fibre in the middle of a vertical tube nitriding furnace. The inner diameter of the furnace is 2.8 cm. The nitriding experiments were performed in an ammonia/hydrogen gas flux (purity: H_2: 99,999 vol.%, NH_3: >99,998 vol.%). The fluxes of both gases were adjusted with mass flow controllers and amounted together 500 ml/min, which corresponds to a linear gas velocity of 1.35 cm/s.

To establish a homogeneous precipitation morphology throughout the thickness of the specimen, pre-nitriding and subsequent de-nitriding treatments were performed prior to the determination of nitrogen-absorption isotherms. To select the appropriate pre-nitriding time, the specimens were nitrided at 580 ºC at a nitriding potential of 0.103 $atm^{-1/2}$ (455 ml/min hydrogen and 45 ml/min ammonia) for three different times: 48, 66 and 72 h. At the end of the nitriding process, the specimen was quenched in water.

After determination of the nitrogen uptake (by weight measurements: see last paragraph of this section), pieces were cut from the specimens and prepared to cross-sections, by subsequent embedding (PolyFast, Buehler GmbH), polishing (last step: 1 µm diamond paste) and etching with

2.0% nital (2.0 vol.% HNO_3 in ethanol) for about 5 s. These cross-sections were characterised by light optical microscopy applying a Leica DMRM microscope (the light micrographs were recorded with a digital camera; Jenoptik Progres 3008) and by measuring hardness-depth profiles obtained by carrying out hardness measurements across the cross-sections of the nitrided specimens using a Leitz Durimet hardness tester, applying a load of 100 g for 12 s. It was found (see section 3.1) that a pre-nitriding time of 48 h suffices for homogeneous nitriding of the whole specimen.

After pre-nitriding, the specimen was de-nitrided in pure H_2 at 470 ºC for 72 h and then cooled to room temperature in a H_2 atmosphere. De-nitriding led to removal of all dissolved and adsorbed (excess) nitrogen, leaving only the nitrogen bonded to Cr in CrN precipitates in the specimen (see section 3.1).

The nitrogen-absorption isotherm was determined using the same nitriding furnace mentioned above. After the consecutive pre- and de-nitriding treatments, the nitrogen-absorption isotherm was determined at temperature well below the pre-nitriding temperature (560°C; cf. table 2) to avoid any change of the precipitation morphology during determination of the nitrogen-absorption isotherm. The nitriding parameters which were used for the determination of the absorption isotherm have been summarised in table 2.

X-ray diffraction analysis performed in this work, and in agreement with such results attained in preceding papers [6, 8], has shown that under the nittriding conditions applied for the pre-nitriding and for the determination of the absorption isotherms that (i) no iron nitrides form at the surface (see also Refs. 3, 4 and 9) and (ii) that only CrN-type precipitates develop (no X-ray diffraction evidence was obtained for the development of Cr_2N-type precipitates).

The nitrogen uptake (or loss; in case of de-nitriding) was determined by weight measurements after and before nitriding (or de-nitriding) using a Mettler microbalance. To determine accurately each weight difference, the average value of five/six weight measurements was taken. The error bars indicated in the results (section 3) represent the maximal deviation from the average value.

Transmission electron microscopy (TEM) studies were performed with the Fe-21.5at.%Cr specimen (1.0 mm thickness), which was nitrided at 580 ºC at a nitriding potential of 0.103 $atm^{-1/2}$ for 48 h. The investigations were performed on planar sections prepared as follows. The specimen was ground from one side down to a thickness of 0.1 mm, implying that the resulting foil consisted fully of nitrided material. After punching discs (diameter 3 mm) electropolishing was performed in an electrolyte of 33 % nitric acid in methanol at a temperature of -40-(-50) °C with a potential of 50 V. TEM was carried out using a Philips CM 20 Twin microscope. The microscope was operated with an accelerating voltage of 200 kV in the nanoprobe mode using a LaB_6 source of electrons.

3. Results and discussion

3.1 *Pre-nitriding and de-nitriding; types of absorbed nitrogen*

The nitrogen uptakes for the thin specimens nitrided at 580 ºC at a nitriding potential of 0.103 $atm^{-1/2}$ for three different times: 48, 66 and 72 h are shown in table 3. It can be concluded that the nitrogen uptake is the same within experimental accuracy for these nitriding times, which indicates that a nitriding time of 48 h suffices for through thickness (homogeneous) nitriding of the specimen. It is not only necessary that saturation of nitrogen uptake has been reached after 48 h of nitriding, but that also the “discontinuous” precipitation morphology occurs across the whole cross-section. Light optical micrographs taken for the specimens nitrided for 48 and 66 h confirm that this is the case indeed (see figure 1). Microhardness measurements support the uniform precipitation morphology across the cross-section: an almost constant hardness is observed over the whole thickness of the specimen (for example, see figure 2 for the specimen nitrided for 48 h). X-ray diffraction analysis performed in this project confirmed the presence of CrN.

After pre-nitriding of a specimen (specimen-2: see table 3) of Fe-21.5at.%Cr alloy, the same specimen was de-nitrided at 470 ºC in pure H_2 gas (500 ml/min) for about 72 h. The nitrogen content which remains in the de-nitrided specimen amounts to 17.29 (± 0.01) at.%. Therefore, the

chromium content in the original Fe-Cr alloy which takes part in the formation of CrN, $[N]_{CrN}$, is ($\frac{17.29 \times 100}{82.71}$ =) 20.90 (± 0.01) at.% (the error margin indicated is based on the experimental error pertaining to the nitrogen content of the de-nitrided specimen determined by weighing (see above)). Chemical analysis of the same alloy indicated a Cr content of about 21.48 (± 0.20) at.% before nitriding (table 1). Hence (21.48 – 20.90 =) 0.58 (± 0.21) at.% Cr (i.e. about 3 – 4% of total chromium content in the alloy) did not take part in the formation of CrN, possibly because it is present in the form of oxides already before nitriding. A similar observation was made for nitrided Fe-1.04at.%Cr [19] and Fe-2.23at.%V alloys [28].

The equilibrium amount of dissolved nitrogen in unstrained pure-iron (ferrite), $[N]_{\alpha}^{0}$, at 580 ºC and at a nitriding potential, r_n, of 0.103 $atm^{-1/2}$ is 0.30 (± 0.004) at.% [28]. Then, the total amount of "excess" nitrogen in the pre-nitrided specimen (r_n = 0.103 $atm^{-1/2}$) can be calculated as follows.

Consider, before nitriding, 100 (Fe + Cr) atoms: i.e. 20.90 Cr atoms + 79.10 Fe atoms. Upon nitriding one has: 20.90 Cr atoms + 20.90 $(N)_{CrN}$ atoms + 79.10 Fe atoms + $\left(\frac{79.10}{100} \times 0.30 = 0.24\right)[N]_{\alpha}^{0}$ atoms + $[N]_{excess}^{total}$ atoms (= 121.14 + $[N]_{excess}^{total}$ atoms); here the symbol "[A]" is used to denote the number of A atoms per 100 (Fe + Cr) atoms. The atom percentage of the total amount of nitrogen ($[N]_{CrN}$ + $[N]_{\alpha}^{0}$ + $[N]_{excess}^{total}$) in the specimen then equals: $\left(\frac{20.90 + 0.24 + [N]_{excess}^{total}}{121.14 + [N]_{excess}^{total}} \times 100\right)$. Pre-nitriding of a Fe-21.5at.%Cr specimen (specimen-2: see table 3) has given an experimental value for this percentage: 18.02. It thus follows that $[N]_{excess}^{total}$ = 0.84 atoms. Therefore, the pre-nitrided specimen has the following composition (now "[A]" denotes the atomic percentage A of the whole specimen)*:

* In the following the concentration "[A]" will be expressed as either "atomic percentage A of the whole specimen" or as "number of A atoms per 100 (Fe + Cr) atoms", which will be indicated explicitly.

$$[\mathrm{Cr}]_{\mathrm{CrN}} = \left(\frac{20.90}{121.14+0.84}\times 100 =\right)\ 17.13\ (\pm\ 0.01)\ \text{at.\%},$$

$$[\mathrm{N}]_{\mathrm{CrN}} = \left(\frac{20.90}{121.14+0.84}\times 100 =\right)\ 17.13\ (\pm\ 0.01)\ \text{at.\%}\ ^{**},$$

$$[\mathrm{Fe}] = \left(\frac{79.10}{121.14+0.84}\times 100 =\right)\ 64.85\ (\pm\ 0.02)\ \text{at.\%},$$

$$[\mathrm{N}]^{0}_{\alpha} = \left(\frac{0.24}{121.14+0.84}\times 100 =\right)\ 0.20\ (\pm\ 0.001)\ \text{at.\%}\ \text{and}$$

$$[\mathrm{N}]^{\mathrm{total}}_{\mathrm{excess}} = \left(\frac{0.84}{121.14+0.84}\times 100 =\right)\ 0.69\ (\pm\ 0.03)\ \text{at.\%};$$

where the error ranges are based on the experimental error in Cr content in the original Fe-Cr alloy which takes part in the formation of CrN (i.e. 20.90 (± 0.01) at.%: see above) and the experimental error in nitrogen content of the specimen after nitriding (table 3).

One might propose that the presence of excess nitrogen is due to the development of (Fe, Cr)N precipitates. However, then the de-nitriding experiment should have led to a nitrogen content higher than the chromium content in the alloy, which is not the case (see above). Hence, the possible explanation of excess nitrogen as due to the development of (Fe, Cr)N precipitates is ruled out.

3.2 *Nitrogen–absorption isotherm*

The nitrogen-absorption isotherm as determined for the pre-nitrided and de-nitrided (cf. section 3.1) Fe-21.5at.%Cr alloy at the nitriding temperature of 560 °C (see section 2) is shown in figure 3 (see also table 4). At constant temperature, the amount of interstitially dissolved nitrogen in the ferrite matrix increases linearly with r_n [3, 4]. Thus the straight-line dependence above level 'B' in figure 3 represents nitrogen dissolved interstitially in the ferrite matrix. Extrapolation of the straight line fitted to the data-points (black squared points in figure 3) of the absorption isotherm to $r_n = 0$

** In the absence of dissolved (mobile excess and equilibrium) and adsorbed nitrogen, it follows: $[\mathrm{N}]_{\mathrm{CrN}} = \left(\frac{20.90}{120.90}\times 100 =\right)$ 17.29 at.% (cf. section 3.2; this is level 'A' in figure 3(a)).

yields the nitrogen level 'B': 17.55 (± 0.02) at.%. The amount of nitrogen required for the formation of stoichiometric CrN has been indicated in figure 3 by level 'A' (nitrogen in de-nitrided specimen): 17.29 (± 0.01) at.% (see footnote in section 3.1 and see also column 4 at $r_n = 0$ in table 5). The difference between level 'B' and level 'A' corresponds with nitrogen taken up in excess of the amounts needed to form the CrN precipitates. According to the earlier analysis of the nitrogen-absorption isotherms recorded for Fe-1.04at.%Cr [19] and Fe-2.23at.%V [28], such nitrogen is adsorbed at the faces of the submicroscopic, coherent nitride platelets (see figure 1 in [28] and the discussion for the current Fe-21.5at.%Cr alloy in section 3.3). The amount of this nitrogen is indicated by $[N]_{interface}$. The composition of a chromium-nitride precipitate with excess nitrogen, $[N]_{interface}$, can be described as CrN_X: where,

$$X = \frac{[N]_{CrN}^{***} + [N]_{interface}}{[N]_{CrN}^{***}} = \frac{\text{Level B}}{\text{Level A}} \qquad (1)$$

The result for X thus obtained is (17.55 (±0.02) / 17.23*** (±0.01) =) 1.019 (± 0.002).

The equilibrium solubility of nitrogen in pure, unstrained iron (ferrite) at temperatures in the range 500 to 570 °C has been determined as function of nitriding potential in [28]. From these results, the following expression can be obtained for the relation between $[N]_\alpha^0$ and T and r_n:

$$[N]_\alpha^0 = \left[\exp\left(19.491 - \frac{10746.1}{T}\right)\right] \cdot r_n \qquad (2)$$

where T, $[N]_\alpha^0$ and r_n are in K, at.% and $Pa^{-1/2}$ respectively. The equilibrium solubilities of nitrogen in ferrite, determined from equation (2), at 560 °C (833 K) for different nitriding potentials have been given in table 4.

The elemental concentrations in the specimen nitrided at 560 °C for different nitriding potentials have been calculated (see results in table 5) using table 4 and applying the procedure described in section 3.1. The values of $[N]_{CrN}$ (and in principle also $[N]_{interface}$) in at.% depend on the nitriding

*** In the de-nitrided specimen, $[N]_{CrN}$ = 17.29 at.% (level 'A' in figure 3(a)). When $[N]_{interface}$ is inserted into the specimen, $[N]_{CrN}$ changes from 17.29 at.% to 17.23 at.%.

potential (see columns 4 (and 7) of table 5; $[N]_{interface}$ is calculated using equation (1), with X is 1.019 (see above result)). In the specimen the *numbers of nitrogen atoms* incorporated in the nitride CrN and adsorbed at the CrN nitride/matrix interface are obviously *in*dependent of the nitriding potential and $[N]_{CrN}$ and $[N]_{interface}$ are independent of the nitriding potential if expressed as the number of nitrogen atoms per 100 (Fe + Cr) atoms (cf. tables 5 and 6). The decrease in levels 'A' and 'B' with increasing nitriding potential in figures 3(a) thus is a straightforward consequence of the nitrogen concentration being expressed in at.%. Hence, for a straightforward interpretation, it is preferred to express the nitrogen concentration in number of N atoms per 100 (Fe + Cr) atoms: figure 3(b). In the previous work on nitrogen-absorption isotherms of Fe-Me alloys (Me = Al, V, Cr, Ti) the distinction between these two ways to express the nitrogen concentration was irrelevant because only a few at.% of alloying element Me were present and the amounts of absorbed nitrogen were correspondingly much smaller.

Subtracting $[N]_{interface}$ from $[N]^{total}_{excess}$ (see column 6 of table 5) gives a value for the amount of excess nitrogen dissolved in the ferrite matrix due to the presence of the precipitate-matrix misfit strain-fields ($[N]_{strain}$: see column 8 of table 5). The subdivision of the total nitrogen uptake into the contributions $[N]_{CrN}$, $[N]_{interface}$, $[N]^0_\alpha$ and $[N]_{strain}$ has been indicated in figure 3.

3.3 *Analysis of "excess" nitrogen uptake in nitrided Fe-Cr alloys*

If coherent precipitation of CrN in the ferrite matrix occurs, enhanced solubility of nitrogen in the ferrite matrix is induced by the precipitate-matrix misfit-strain. This enhanced nitrogen solubility, $[N]_{strain}$, can be calculated using the model described in section 3 of [22]. The thus calculated value of $[N]_{strain}$ (expressed as number of N atoms per 100 Fe atoms of the ferrite matrix) is shown as function of the chromium content of Fe-Cr alloy nitrided at 560 ºC and at a nitriding potential of 0.140 $atm^{-1/2}$ (cf. figure 3) in figure 4. Evidently, $[N]_{strain}$ increases with increasing [Cr]

to, hypothetically, very large values for chromium concentrations above 10 at.%. In reality, an only small amount of mobile "excess" dissolved nitrogen, i.e. $[N]_{strain}$, has been determined for the present Fe-21.5at.%Cr alloy: 0.37 at.% N = 0.45 N atoms per 100 (Fe + Cr) atoms = 0.57 N atoms per 100 Fe atoms (cf. column 8 in table 5; column 5 in table 6), which is in fact much less than the value expected from figure 4 if "coherent" precipitation of CrN in the ferrite matrix would have occurred for all CrN. Also the amount of immobile "excess" nitrogen represented by the value of X is very small: X = 1.02 (cf. section 3.2), as compared to X = 1.24 for the Fe-1.04at.%Cr [19] alloy; in the latter case the nitrided zone exhibits (only) the "continuous" precipitation morphology.

The above results can be understood as a consequence of the almost immediate transition, occurring upon nitriding the Fe-21.5at.%Cr alloy, from coherent, submicroscopical CrN precipitates to the discontinuously coarsened lamellar microstructure, which process involves loosing the capacity for excess nitrogen uptake (the Fe-1.04at.%Cr alloy maintains the submicroscopical, continuous precipitation morphology during nitriding and thus can unfold the full capacity for excess nitrogen uptake).

The spontaneous / immediate occurrence of the discontinuous coarsening reaction in Fe-21.5at.%Cr alloy upon nitriding can be understood recognising the enormous amount of misfit stress induced in the matrix if all Cr precipitates as coherent CrN: the relaxation of such pronounced long-range strain fields in association with the great reduction in precipitate/matrix interfacial area provides a very large driving force for the occurrence of discontinuous coarsening for nitrided, in particular, high-chromium iron-based alloys.

If a specimen of Fe-21.5at.%Cr alloy is not relatively long and through nitrided, a larger amount of excess nitrogen is observed in the nitrided part of the specimen (~ 3 at.% excess nitrogen [8] versus 0.69 at.% (cf. section 3.1); X = 1.11 [8] versus 1.02 (cf. section 3.2); specimens nitrided under the same conditions). This can be understood as follows: most excess nitrogen, that has been taken up before the discontinuous coarsening reaction occurs, has been able to escape from the thin,

through (homogeneously) nitrided specimen upon discontinuous coarsening and continued exposure to the nitriding atmosphere at the nitriding temperature, whereas for the relatively short nitrided (thick, not through nitrided) specimen with a surface adjacent nitrided zone [8], this has not been possible to realize already.

If all Cr content in Fe-21.5at.%Cr alloy would have participated in the discontinuous coarsening upon nitriding, one should expect negligible amounts of excess nitrogen. This is not the case (see results indicated above). It is suggested that not all Cr is involved in the discontinuous coarsening: the discontinuous coarsening front sweeps through nitrided grains (note the large driving force for discontinuous coarsening in high alloyed Fe-Cr alloys, as discussed above) before all Cr has been precipitated as nitride. This remaining part of Cr dissolved in ferrite then precipitates upon continued nitriding as coherent chromium-nitride platelets in the ferrite lamellae of the discontinuously coarsened microstructure, i.e. after discontinuous coarsening has occurred.*

Indeed, TEM analysis (see further) performed in this project (cf. section 2) shows the occurrence of CrN platelets in such ferrite lamellae in the discontinuously coarsened microstructure of nitrided Fe-Cr alloy (figure 5). TEM examination of the specimen (1.0 mm thickness) nitrided at 580 ºC at a nitriding potential of 0.103 $atm^{-1/2}$ for 48 h demonstrated that the discontinuous coarsening led to the formation of a lamellar structure (see figures 5(a) and (b)). The selected area electron diffraction pattern (SADP) recorded from the nitride lamella indicated in figure 5(a) with the number "1" allowed identification of this lamella as CrN. A ferrite lamellae appears with rich contrast in figure 5(b) (see also at number "2" in figure 5(a)). A peculiar feature in the bright field images is the presence of finely dispersed platelets within the ferrite lamellae. The SADP corresponding to an

* Thus the value of X determined in section 3.2, as an average for all CrN precipitates in the specimen, should in fact be related with the minor formation of coherent CrN precipitates and then is larger accordingly.

area within the α-Fe lamella shown in figure 5(b) shows α-Fe reflections compatible with an $[100]_{\alpha\text{-Fe}}$ electron-beam zone axis and CrN reflections compatible with a Bain-type orientation relationship of the CrN precipitates with the α-Fe matrix ($\{001\}_{\alpha\text{-Fe}} \parallel \{001\}_{CrN}$; $<100>_{\alpha\text{-Fe}} \parallel <110>_{CrN}$; for a similar observation for AlN precipitates in α-Fe, see figure 2 in [29]) (figure 5(c)). Some further reflections can be discerned as well and are ascribed to double diffraction and/or metal oxides. Dark field images of two 020–type CrN reflections, pertaining to two variants of the Bain-type orientation relationship, and marked by circles in figure 5(c), are shown in figures 5(d) and (e). Obviously, the platelets of the two orientation-relationship variants are oriented mutually perpendicularly. Further, it is observed that strong variations occur in the diffracted intensity in the diffraction-contrast images of single platelets. A similar observation has been made recently for VN platelets in an α-Fe matrix, which could be shown to be due to local bending and disruptions of lattice integrity in the VN precipitates as a likely consequence of compliance with the strongly varying (misfit-strain) fields during precipitate lengthening [30].

The (coherent) nitride platelets in the ferrite lamellae are responsible for the observed excess nitrogen in nitrided discontinuously coarsened high chromium Fe-Cr alloys. The fraction of Cr in the alloy which is involved in the (delayed) formation of such coherent nitride platelets in the ferrite lamellae has been estimated as follows: The amount of $[N]_{strain}$ in the Fe-21.5at.%Cr alloy nitrided at 560 ºC and at a nitriding potential of 0.140 $atm^{-1/2}$ is 0.37 at.%, i.e. ($\frac{[N]_{strain} \times 100}{[Fe]}$ =) 0.57 N atoms per 100 atoms of Fe (cf. table 5). Then, using the calculated results shown in figure 4, it follows that the Cr content in the Fe-21.5at.%Cr alloy involved in the formation of coherent precipitates in the ferrite lamellae is (at most) about 3.8 at.% (This result holds for X=1 (see figure 4); for larger values of X (cf. footnote in this section) somewhat smaller values for the Cr content incorporated in coherent nitride precipitates are obtained (see inset in Fig. 4)

4. Conclusions

- Nitriding of Fe-21.5at.%Cr alloy leads to a "discontinuous" nitride precipitation morphology in the entire nitrided zone and the presence of a minor fraction of coherent nitride precipitates within the ferrite lamellae of the "discontinuous" precipitation morphology.
- Mass changes recorded after pre-nitriding (in NH_3 / H_2 gas mixture) and after subsequent de-nitriding (in pure H_2 gas) demonstrate that the composition of the nitride precipitates formed is given by the formulae CrN, and not (Fe, Cr)N: Fe is not incorporated significantly in the nitride precipitates.
- For highly alloyed Fe-Me alloys, evaluation of the total nitrogen uptake requires expressing the amounts of the various types of absorbed nitrogen as the number of N atoms per 100 (Fe + Me) atoms.
- Upon nitriding Fe-21.5at.%Cr alloy more nitrogen is taken up than necessary for precipitation of all chromium as nitride and equilibrium saturation with nitrogen of the ferrite matrix. Analysis of the nitrogen-absorption isotherm reveals two kinds of this "excess nitrogen": (a) immobile excess nitrogen (adsorbed at precipitate/matrix interface) and (b) mobile excess nitrogen (dissolved interstitially in the ferrite matrix).
- The observation of excess nitrogen in discontinuously coarsened nitrided Fe-Cr alloy is unexpected: occurrence of excess nitrogen has been ascribed before to the occurrence of submicroscopical, coherent nitride precipitates, which is incompatible with a discontinuously coarsened microstructure.
- This work has shown that part of the chromium in the specimen is not taken up in the CrN lamellae but has precipitated as tiny CrN platelets within the ferrite lamellae; these precipitates are responsible for the uptake of excess nitrogen. Quantitative model-based analysis shows that (at most) about 3.8 at.% Cr, of the 21.5 at.% Cr in the alloy has precipitated as small nitride platelets within the ferrite lamellae.

- The chromium precipitating in the ferrite lamellae, after the discontinuous coarsening upon continued nitriding, is the chromium not already precipitated as CrN at the moment the discontinuous coarsening front sweeps through the (not yet completely, i.e. up to saturation) nitrided grains.

References

[1] *Source Book on Nitriding*, American Society for Metals, Metals Park, Ohio, 1977.

[2] *ASM Handbook: Heat Treating*, ASM International, Vol. 4, Metals Park, Ohio, 1991.

[3] E.J. Mittemeijer and J.T. Slycke, Surface Engineering 12 (1996), p. 152.

[4] E.J. Mittemeijer and M.A.J. Somers, Surface Engineering 13 (1997), p. 483.

[5] P.M. Hekker, H.C.F. Rozendaal and E.J. Mittemeijer, Journal of Materials Science 20 (1985), p. 718.

[6] R.E. Schacherl, P.C.J. Graat and E.J. Mittemeijer, Z. Metalld. 93 (2002), p. 468.

[7] R.E. Schacherl, P.C.J. Graat and E.J. Mittemeijer, *Nitriding of Fe-Cr alloys with high chromium contents*, in *Proceedings of the Symposium on Nitriding*, J. Grosch and E.J. Mittemeijer, editors, Arbeitsgemeinschaft Wärmebehandlung und Werkstofftechnik (AWT), Schlangenbad, Germany, 2002. p. 51.

[8] R.E. Schacherl, P.C.J. Graat and E.J. Mittemeijer, Metall. Mater. Trans. 35A (2004), p. 3387.

[9] S.S. Hosmani, R.E. Schacherl and E.J. Mittemeijer, Materials Science and Technology 21 (2005), p. 113.

[10] M. Sennour, P.H. Jouneau and C. Esnouf, Journal of Materials Science 39 (2004) p. 4521.

[11] M. Sennour, C. Jacq and C. Esnouf, Journal of Materials Science 39 (2004), p. 4533.

[12] B. Mortimer, P. Grieveson and K.H. Jack, Scandinavian Journal of Metallurgy 1 (1972), p. 203.

[13] J. Takada, Y. Ohizumi, H. Miyamura, H. Kuwahara, S. Kikuchi and I. Tamura, Journal of Materials Science 21 (1986), p. 2493.

[14] W.M. Small, Scripta Metallurgica 24 (1990), p. 107.

[15] C. Alves, J. de Anchieta Rodrigues and A. Eduardo Martinelli, Mater. Sci. Eng. 279A (2000), p. 10.

[16] K. Gemma, T. Ohtsuka, T. Fujiwara and M. Kawakami, Journal of Materials Science 36 (2001), p. 5231.

[17] P. Schaaf, Progress in Materials Science 47 (2002), p. 1.

[18] G. Miyamoto, A. Yonemoto, Y. Tanaka, T. Furuhara and T. Maki, Acta Materialia 54 (2006), p. 4771.

[19] S.S. Hosmani, R.E. Schacherl and E.J. Mittemeijer, Journal of Materials Science (2008), in press. DOI: 10.1007/s10853-008-2473-9

[20] D.B. Williams and E.P. Butler, Int. Met. Rev. 26 (1981), p. 153.

[21] N.E. Vives Díaz, R.E. Schacherl and E.J. Mittemeijer, International Journal of Materials Research (2008), in press.

[22] M.A.J. Somers, R.M. Lankreijer and E.J. Mittemeijer, Phil. Mag. 59A (1989), p. 353.

[23] M.H. Biglari, C.M. Brakman, E.J. Mittemeijer and S. van der Zwaag, Phil. Mag. 72A (1995), p. 931.

[24] D.H. Jack, Acta Metall. 24 (1976), p. 137.

[25] H.H. Podgurski and F.N. Davis, Acta Metall. 29 (1981), p. 1.

[26] D.S. Rickerby, S. Henderson, A. Hendry and K.H. Jack, Acta Metall. 34 (1986), p. 1687.

[27] H.H. Podgurski, R.A. Oriani and N.A. Davis, with Appendix by J.C.M. Li and Y.T. Chou, Trans. Metall. Soc. AIME 245 (1969), p. 1603.

[28] S.S. Hosmani, R.E. Schacherl and E.J. Mittemeijer, Acta Materialia 54 (2006), p. 2783.

[29] M.H. Biglari, C.M. Brakman and E.J. Mittemeijer, Phil. Mag. 72A (1995), p. 1281.

[30] N.E. Vives Díaz, S.S. Hosmani, R.E. Schacherl and E.J. Mittemeijer, Submitted for publication.

All Tables

Table 1: Amounts of chromium and light element impurities for the Fe-21.5at.%Cr alloy used in this work.

Cr (wt.%)	Cr (at.%)	O (wt.%)	N (wt.%)	C (wt.%)	S (wt.%)	Fe
20.3 ± 0.2	21.48 ± 0.20	0.0170 ± 0.0010	< 0.0010	0.0096 ± 0.0007	< 0.0010	bal.

Table 2: Summary of the nitriding parameters used for determination of the nitrogen-absorption isotherm for the Fe-21.5at.%Cr alloy.

pre- and de-nitrided (see section 2) specimen	determination of absorption isotherms				
	temperature (°C)	time (h)	NH_3 (ml/min)	H_2 (ml/min)	r_n ($atm^{-1/2}$)
Fe-21.5at.%Cr pre-nitrided at 580 °C (in a NH_3 / H_2 atmosphere); **de-nitrided at 470 °C** (in a pure H_2 atmosphere)	560	72	25	475	0.054
			35	465	0.078
			50	450	0.117
			58	442	0.140

Table 3: Nitrogen uptake by Fe-21.5at.%Cr specimens (thickness ≈ 0.30 mm each) nitrided at 580 °C, at a nitriding potential of 0.103 $atm^{-1/2}$ for different nitriding times.

nitriding time (h)	nitrogen uptake in Fe-21.5at.%Cr foil (at.%)
48 (specimen-1)	17.96 (± 0.01)
48 (specimen-2)	18.02 (± 0.02)
66 (specimen-3)	17.98 (± 0.01)

72 (specimen-4)	17.95 (± 0.02)

Table 4: Nitrogen uptake in pre-nitrided and de-nitrided specimen of Fe-21.5at.%Cr alloy nitrided at 560 ºC at different nitriding potentials. Values for nitrogen uptake in unstrained pure Fe at 560 ºC for different nitriding potentials have been calculated using equation (2).

nitriding potential, r_n ($atm^{-1/2}$)	**total nitrogen uptake (at.%)**	**total nitrogen uptake (N atoms per 100 atoms of Fe + Cr)**	**nitrogen uptake in unstrained pure-Fe at 560 °C (see equation (2)) (at.%)**
0	17.55 (± 0.02) [#]	21.29 (± 0.02)	0
0.054	17.72 (± 0.01)	21.55 (± 0.01)	0.12
0.078	17.81 (± 0.02)	21.68 (± 0.02)	0.18
0.117	17.93 (± 0.01)	21.85 (± 0.01)	0.27
0.140	18.03 (± 0.01)	22.00 (± 0.01)	0.32

[#] Estimate: extrapolation of the straight line fitted to the data-points (black squared points in figure 3(b)) to $r_n = 0$ yields the nitrogen level 'B' (21.29 N atoms per 100 (Fe + Cr) atoms = 17.55 at.% N; see also section 3.2).

Table 5: The elemental concentrations (columns 2 to 6) of the Fe-21.5at.%Cr specimen nitrided at 560 °C at different nitriding potentials calculated using table 4 and the calculation procedure described in section 3.1. For $r_n = 0$, the total excess nitrogen ($[N]^{total}_{excess}$ **:** column 6 at $r_n = 0$) reduces to the amount of nitrogen adsorbed at the precipitate/matrix interface ($[N]_{interface}$). The value of $[N]_{interface}$ at different nitriding potentials has been calculated (column 7) using equation (1), with X = 1.019. Subtracting $[N]_{interface}$ (column 7) from $[N]^{total}_{excess}$ (column 6) gives the amount of excess nitrogen dissolved in the ferrite matrix as caused by the precipitate-matrix misfit-strain field, $[N]_{strain}$ (column 8). The concentrations are expressed as at.% for the *whole* specimen.

(1) **nitriding potential, r_n ($atm^{-1/2}$)**	**(2)** [Fe] **(at.%)**	**(3)** $[Cr]_{CrN}$ **(at.%)**	**(4)** $[N]_{CrN}$ **(at.%)**	**(5)** $[N]^0_\alpha$ **(at.%)**	**(6)** $[N]^{total}_{excess}$ **(at.%)**	**(7)** $[N]_{interface} = [N]_{CrN}$ *(X-1) **(at.%)**	**(8) = (6) – (7)** $[N]_{strain} = [N]^{total}_{excess} - [N]_{interface}$ **(at.%)**
0	65.42 † (± 0.01)	17.29 † (± 0.01)	17.29 † (± 0.01)	0	0.32 ‡ (± 0.03)	0.32 ‡ (± 0.03)	0
0.054	65.08 (± 0.02)	17.20 (± 0.01)	17.20 (± 0.01)	0.08	0.45 (± 0.02)	0.32 (± 0.01)	0.13 (± 0.03)
0.078	65.01 (± 0.02)	17.18 (± 0.01)	17.18 (± 0.01)	0.12	0.52 (± 0.03)	0.32 (± 0.01)	0.20 (± 0.04)
0.117	64.92 (± 0.02)	17.15 (± 0.01)	17.15 (± 0.01)	0.18	0.60 (± 0.02)	0.32 (± 0.01)	0.28 (± 0.03)
0.140	64.84 (± 0.02)	17.13 (± 0.01)	17.13 (± 0.01)	0.21	0.69 (± 0.02)	0.32 (± 0.01)	0.37 (± 0.03)

† These percentages hold if only Fe, Cr_{CrN} and N_{CrN} are present (level 'A' in figure 3).

‡ These values pertain to level 'B' (figure 3); after de-nitriding: 0 at.% (as holds for level 'A'; figure 3).

Table 6: The concentrations of nitrogen ($[N]_{CrN}$, $[N]_{\alpha}^{0}$, $[N]_{interface}$, $[N]_{strain}$) in number of N atoms per 100 (Fe + Cr) atoms in the specimen. The results shown are based on the data given in table 5. Errors in (different types of) nitrogen concentrations are based on the errors in corresponding nitrogen concentrations given in table 5.

(1) **nitriding potential, r_n ($atm^{-1/2}$)**	**(2)** $\frac{[N]_{CrN} \times 100}{[Fe]+[Cr]}$	**(3)** $\frac{[N]_{\alpha}^{0} \times 100}{[Fe]+[Cr]}$	**(4)** $\frac{[N]_{interface} \times 100}{[Fe]+[Cr]}$ =	**(5)** $\frac{[N]_{strain} \times 100}{[Fe]+[Cr]}$
0	20.90 (± 0.01)	0	0.39 (± 0.03)	0
0.054	20.90 (± 0.01)	0.10	0.39 (± 0.01)	0.16 (± 0.03)
0.078	20.90 (± 0.01)	0.15	0.39 (± 0.01)	0.24 (± 0.04)
0.117	20.90 (± 0.01)	0.22	0.39 (± 0.01)	0.34 (± 0.03)
0.140	20.90 (± 0.01)	0.26	0.39 (± 0.01)	0.45 (± 0.03)

Figure captions

Figure 1: Light optical micrographs of the etched cross-sections of Fe-21.5at.%Cr specimens nitrided at 580 ºC at a nitriding potential of 0.103 $atm^{-1/2}$ for (a) 48 h and (b) 66 h.

Figure 2: Microhardness-depth profile across the whole cross-section of an Fe-21.5at.%Cr specimen nitrided at 580 ºC for 48 h at a nitriding potential of 0.103 $atm^{-1/2}$ (a). Light optical micrograph showing the corresponding Vickers-indentations is presented in (b).

Figure 3: Nitrogen-absorption isotherm as determined for pre-nitrided and de-nitrided Fe-21.5at.%Cr alloy at 560 ºC for different nitriding potentials (see table 2) for the case that the nitrogen content is expressed in terms of either (a) at.% or (b) nitrogen atoms per 100 atoms of Fe + Cr (for error range pertaining to the data points, see table 4). The linear fit (dashed line) to the measured data (black squared points) has been extrapolated to the intercept at $r_n = 0$ which gives the nitrogen level 'B'. Level 'A' indicates the amount of nitrogen required for the formation of stoichiometric CrN, i.e. $[N]_{CrN}$. The sub-division of total nitrogen uptake (at different nitriding potentials) into: nitrogen incorporated in CrN ($[N]_{CrN}$), nitrogen adsorbed at precipitate/matrix interface ($[N]_{interface}$), nitrogen dissolved in unstrained ferrite ($[N]_{\alpha}^{0}$) and excess nitrogen dissolved in the ferrite matrix due to the precipitate-matrix misfit strain ($[N]_{strain}$) has been indicated.

Figure 4: The calculated (hypothetical) amount of nitrogen dissolved in the ferrite matrix in the presence of precipitate-matrix long-range misfit-strain fields for Fe-Cr alloy nitrided at 560 ºC at a nitriding potential of 0.140 $atm^{-1/2}$ as function of chromium content of the alloy. The dashed-curve pertains to CrN_X with X = 1 (i.e. no nitrogen adsorbed at precipitate/matrix interface); the solid - curve pertains to CrN_X with X = 1.019, as observed for the present experiments, and in the case of complete elastic accommodation of the misfit (i.e. f = 1.0; for details see [22]).

Figure 5: (a) TEM micrograph (bright field) showing CrN lamellae (see number "1") and α-Fe lamellae (see number "2") in a lamellar colony in the discontinuously coarsened microstructure of the Fe-21.5at.%Cr alloy nitrided at 580 ºC at a nitriding potential of 0.103 $atm^{-1/2}$ for 48 h. Tiny CrN nitride platelets are visible within the ferrite lamellae. (b) TEM micrograph (bright field) showing a ferrite lamella (with rich diffraction contrast due to different sets of CrN platelets corresponding to different variants of the Bain-type orientation relationship); (c) Selected area diffraction pattern of region within the ferrite lamella shown in (b) ($[100]_{\alpha\text{-Fe}}$ electron-beam axis / zone axis). Diffraction spots of the CrN platelets can be observed in accordance with variants of the Bain-type orientation relationship: $\{001\}_{\alpha\text{-Fe}} \parallel \{001\}_{CrN}$; $<100>_{\alpha\text{-Fe}} \parallel <110>_{CrN}$; see also [12, 22, 29]. The reflections used for dark-field imaging are marked by circles: (d) dark field image of the 020 CrN reflection marked "(I)" in (c) and (d) dark field image of the 020 CrN reflection marked "(II)" in (c).

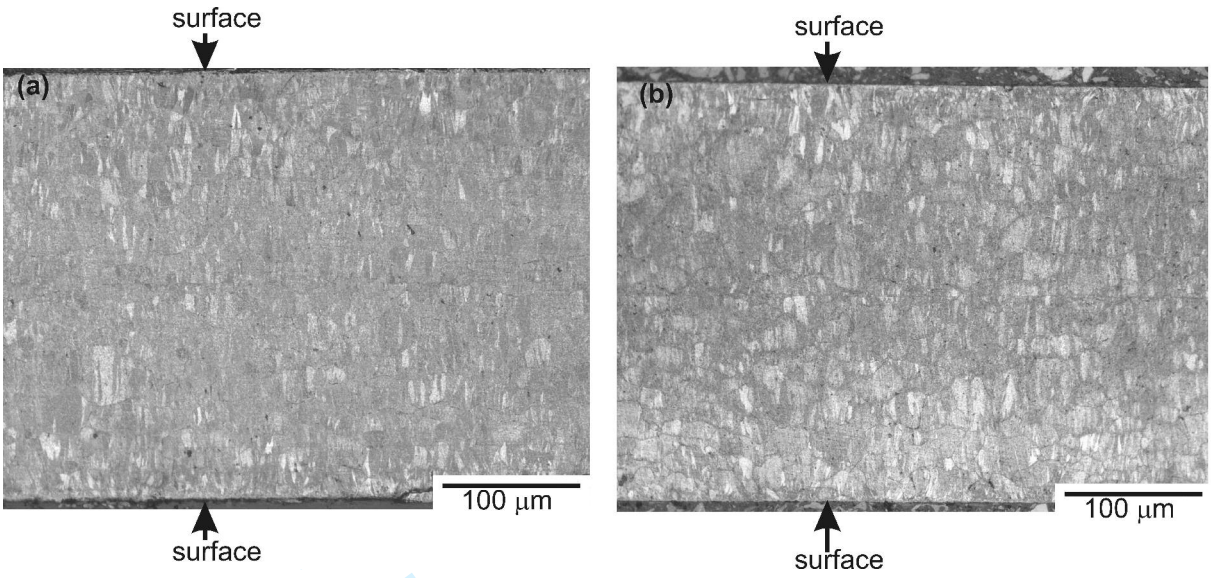

Figure 1: Light optical micrographs of the etched cross-sections of Fe-21.5at.%Cr specimens nitrided at 580 ºC at a nitriding potential of 0.103 $atm^{-1/2}$ for (a) 48 h and (b) 66 h.

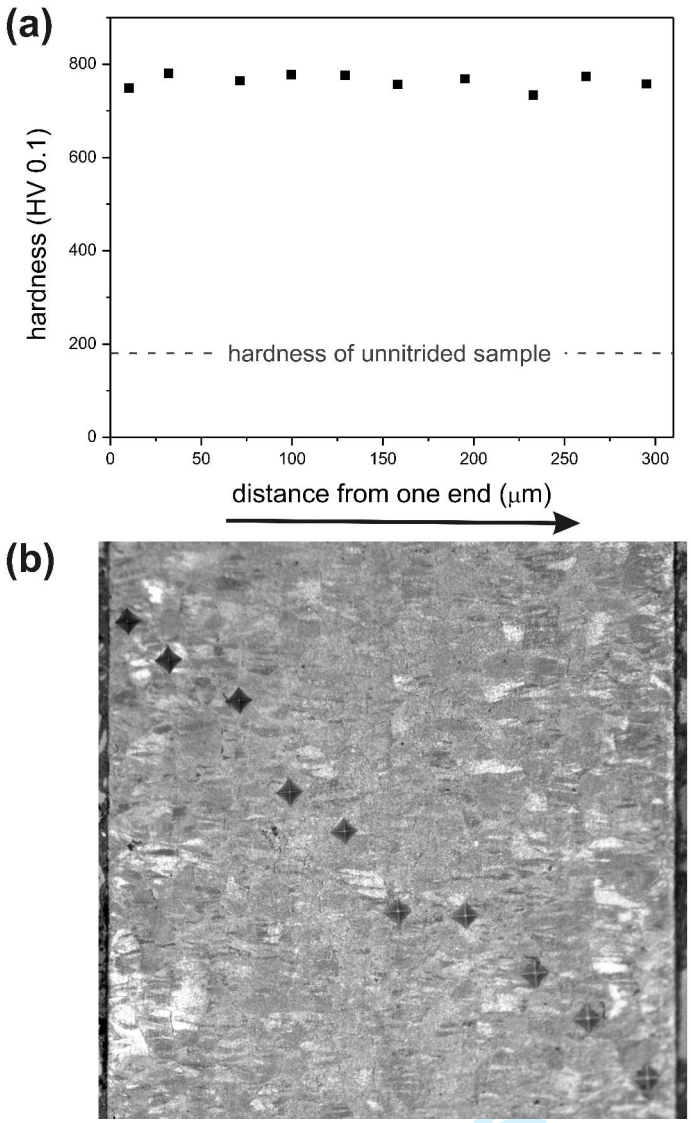

Figure 2: Microhardness-depth profile across the whole cross-section of an Fe-21.5at.%Cr specimen nitrided at 580 ºC for 48 h at a nitriding potential of 0.103 $atm^{-1/2}$ (a). Light optical micrograph showing the corresponding Vickers-indentations is presented in (b).

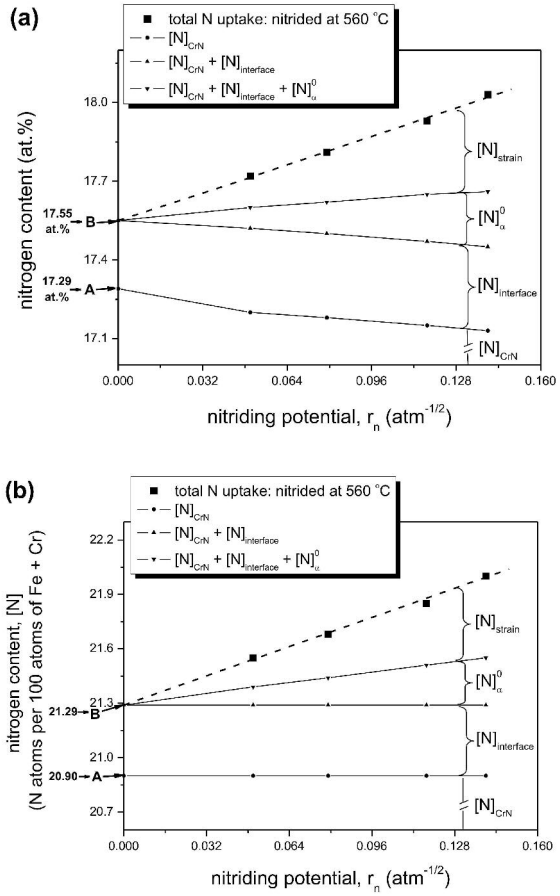

Figure 3: Nitrogen-absorption isotherm as determined for pre-nitrided and de-nitrided Fe-21.5at.%Cr alloy at 560 ºC for different nitriding potentials (see table 2) for the case that the nitrogen content is expressed in terms of either (a) at.% or (b) nitrogen atoms per 100 atoms of Fe + Cr (for error range pertaining to the data points, see table 4). The linear fit (dashed line) to the measured data (black squared points) has been extrapolated to the intercept at r_n = 0 which gives the nitrogen level 'B'. Level 'A' indicates the amount of nitrogen required for the formation of stoichiometric CrN, i.e. $[N]_{CrN}$. The sub-division of total nitrogen uptake (at different nitriding potentials) into: nitrogen incorporated in CrN ($[N]_{CrN}$), nitrogen adsorbed at precipitate/matrix interface ($[N]_{interface}$), nitrogen dissolved in unstrained ferrite ($[N]^0_\alpha$) and excess nitrogen dissolved in the ferrite matrix due to the precipitate-matrix misfit strain ($[N]_{strain}$) has been indicated.

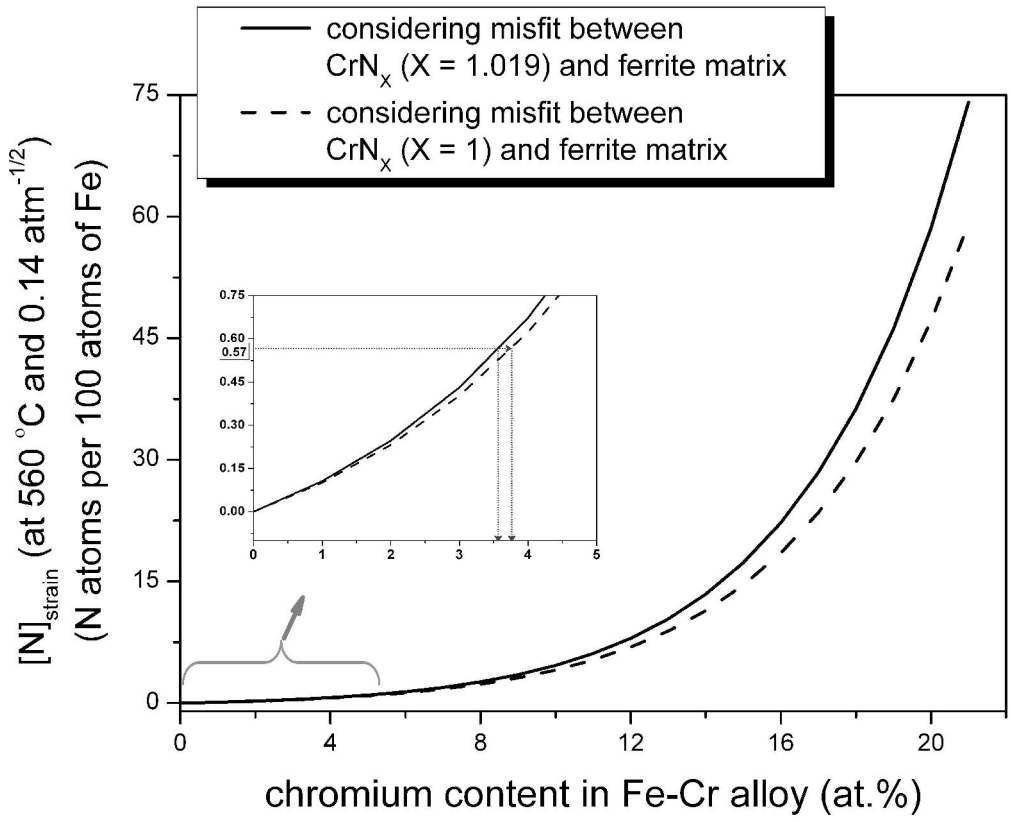

Figure 4: The calculated (hypothetical) amount of nitrogen dissolved in the ferrite matrix in the presence of precipitate-matrix long-range misfit-strain fields for Fe-Cr alloy nitrided at 560 ºC at a nitriding potential of 0.140 atm$^{-1/2}$ as function of chromium content of the alloy. The dashed-curve pertains to CrN_X with X = 1 (i.e. no nitrogen adsorbed at precipitate/matrix interface); the solid -curve pertains to CrN_X with X = 1.019, as observed for the present experiments, and in the case of complete elastic accommodation of the misfit (i.e. f = 1.0; for details see [22]).

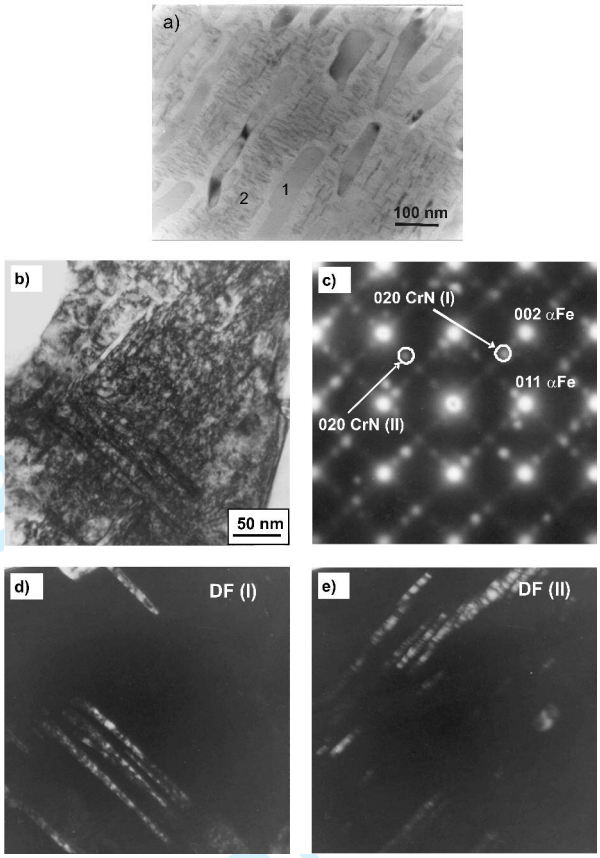

Figure 5: (a) TEM micrograph (bright field) showing CrN lamellae (see number "1") and α-Fe lamellae (see number "2") in a lamellar colony in the discontinuously coarsened microstructure of the Fe-21.5at.%Cr alloy nitrided at 580 °C at a nitriding potential of 0.103 $atm^{-1/2}$ for 48 h. Tiny CrN nitride platelets are visible within the ferrite lamellae. (b) TEM micrograph (bright field) showing a ferrite lamella (with rich diffraction contrast due to different sets of CrN platelets corresponding to different variants of the Bain-type orientation relationship); (c) Selected area diffraction pattern of region within the ferrite lamella shown in (b) ($[100]_{\alpha\text{-Fe}}$ electron-beam axis / zone axis). Diffraction spots of the CrN platelets can be observed in accordance with variants of the Bain-type orientation relationship: $\{001\}_{\alpha\text{-Fe}} \parallel \{001\}_{CrN}$; $<100>_{\alpha\text{-Fe}} \parallel <110>_{CrN}$; see also [12, 22, 29]. The reflections used for dark-field imaging are marked by circles: (d) dark field image of the 020 CrN reflection marked "(I)" in (c) and (d) dark field image of the 020 CrN reflection marked "(II)" in (c).